

Coverage Guided Testing for Recurrent Neural Networks

Wei Huang¹, Youcheng Sun², James Sharp³, Wenjie Ruan⁴, Jie Meng⁵, and Xiaowei Huang¹

Abstract—Recurrent neural networks (RNNs) have been applied to a broad range of applications such as natural language processing, drug discovery, and video recognition. This paper develops a coverage-guided testing approach for a major class of RNNs – long short-term memory networks (LSTMs). We start from defining a family of three test metrics that are designed to quantify not only the values but also the temporal relations (including both step-wise and bounded-length) learned through LSTM’s internal structures. While testing, random mutation enhanced with the coverage knowledge, i.e., targeted mutation, is designed to generate test cases. Based on these, we develop the coverage-guided testing tool TESTRNN. To our knowledge, this is the first time structural coverage metrics are used to test LSTMs.

We extensively evaluate TESTRNN with a variety of LSTM benchmarks. Experiments confirm that there is a positive correlation between adversary rate and coverage rate, an evidence showing that the test metrics are valid indicators of robustness evaluation. Also, we show that TESTRNN effectively captures erroneous behaviours in RNNs. Furthermore, meaningful information can be collected from TESTRNN for users to understand what the testing results represent. This is in contrast to most neural network testing works, and we believe TESTRNN is an important step towards interpretable neural network testing.

Index Terms—RNNs, coverage guided testing, coverage metrics, test case generation.

I. INTRODUCTION

Since the discovery of adversarial examples in deep feed-forward neural networks (FNNs), particularly convolutional neural networks (CNNs) for image classification [46], the robustness of deep learning applications has been studied from different perspectives, including attack and defence [6], [31], verification [25], [23], and testing [35], [44], [29]. Erroneous behaviours also occur in RNNs and undermine its robustness [2]. Different from CNNs, RNNs exhibit particular challenges, due to more complex internal structures and their processing of sequential inputs with a temporal semantics, with the support of internal memory components. Meanwhile, popular deep learning libraries such as TensorFlow do not support direct access to an RNN’s internal data flow.

As illustrated in Fig. 1, a generic RNN layer takes an input x , updates its internal state c , and generates an output h . Other structural components may be required for specific RNNs. Given a sequential input $\{x_t\}_{t=1}^n$, the RNN layer will be unfolded with respect to the size n of the input, and therefore

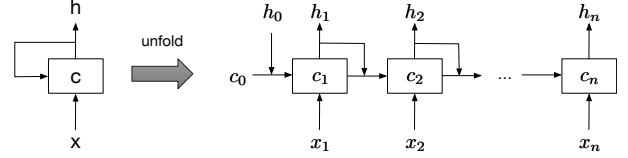


Fig. 1: A simple, generic recurrent layer

each structural component has a corresponding sequence of representations, for example $\{h_t\}_{t=1}^n$ as in Fig. 1. Such a sequence of representations form a temporal evolution.

Coverage-guided testing has been shown a great success in software fault detection. It has been extended to work with FNNs in recent work such as [35], [49], [29], [43], [44], where a collection of FNN coverage metrics can be found. These metrics are based on the structural data flow in the FNNs, such as the neurons’ activations [35], [29], the relation between neurons in neighboring layers [43], [44], etc. Unfortunately, these metrics are insufficient for RNNs because they do not work with the internal structures of RNNs and, more importantly, the most essential ingredient of RNNs – the temporal relation – is not considered. Hence, new test metrics are needed to take into account the additional structures and temporal semantics.

a) Contributions: In this paper, we focus on long short-term memory networks (LSTMs), which is the most important class of RNNs. For an LSTM cell, its structural components include three functional gates f, i, o , a cell state c , and an output h , all of which can be represented as a real vector for any given time t . We design three LSTM structural coverage metrics, namely boundary coverage (BC), step-wise coverage (SC) and temporal coverage (TC). Simply speaking, BC is to quantify the values of the information abstracted from the structural components of LSTM cells, while SC and TC are to quantify their internal temporal semantics, for step-wise and multi-step with bounded-length, respectively. We remark that, while we focus on LSTMs in this paper, these test metrics can easily be extended to work with other classes of RNNs.

Our tool TESTRNN uses the coverage knowledge to guide the test case generation. Initially, a random mutation is taken to generate test cases. Once the un-targeted randomisation has been hard to improve the coverage rate, a targeted mutation by considering the distance to the satisfaction of un-fulfilled test conditions is taken to generate corner test cases.

We conduct an extensive set of experiments over a diverse set of LSTM benchmarks to confirm the utility of the proposed coverage-guided LSTM testing approach with the following

¹Wei Huang, and Xiaowei Huang are with University of Liverpool, UK.

²Youcheng Sun is with Queen’s University Belfast, UK

³James Sharp is with Defence Science and Technology Laboratory, UK

⁴Wenjie Ruan is with Lancaster University, UK

⁵Jie Meng is with Loughborough University, UK

conclusions.

- 1) There is a positive correlation between adversary rate, i.e., the percentage of adversarial examples in the generated test cases, and the coverage rate, i.e., the percentage of test conditions satisfied by the generated test cases. This is a strong evidence showing that our test metrics can be meaningfully taken as **valid indicators** of robustness evaluation, countering a recent argument made in [28], [13] for CNN structural coverage testing.
- 2) The test metrics are effective in **capturing erroneous behaviours** of LSTMs. They are also shown to complement with each other, which aligns with our view of achieving **test diversity**.
- 3) The developed TESTRNN tool is efficient and effective in achieving **high coverage rates**.
- 4) Semantic meanings behind the test metrics can in turn help users understand the learning mechanism of LSTM model, a step towards **interpretable** LSTM testing.

II. RNN PRELIMINARIES

Feedforward neural networks (FNNs) model a function $\phi : X \rightarrow Y$ that maps from input domain X to output domain Y : given an input $x \in X$, it outputs the prediction $y \in Y$. For a sequence of inputs x_1, \dots, x_n , an FNN ϕ considers each input individually, that is, $\phi(x_i)$ is independent from $\phi(x_{i+1})$.

By contrast, recurrent neural networks (RNNs) are designed to handle sequential data. An RNN contains at least one recurrent layer, as depicted in Fig. 1, that processes an input sequence by iteratively taking inputs one by one. A recurrent layer can be modeled as a function $\psi : X' \times C \times Y' \rightarrow C \times Y'$ such that $\psi(x_t, c_{t-1}, h_{t-1}) = (c_t, h_t)$ for $t = 1 \dots n$, where t denotes the t -th time step, c_t is the cell state used to represent the intermediate memory and h_t is the output of the t -th time step. More specifically, the recurrent layer takes three inputs: x_t at the current time step, the prior memory state c_{t-1} and the prior cell output h_{t-1} ; consequently, it updates the current cell state c_t and outputs current h_t .

RNNs differ from each other given their respective definitions, i.e., internal structures, of recurrent layer function ψ , of which long short-term memory (LSTM) in Equation (1) is the most popular and commonly used one.

$$\begin{aligned} f_t &= \sigma(W_f \cdot [h_{t-1}, x_t] + b_f) \\ i_t &= \sigma(W_i \cdot [h_{t-1}, x_t] + b_i) \\ c_t &= f_t * c_{t-1} + i_t * \tanh(W_c \cdot [h_{t-1}, x_t] + b_c) \\ o_t &= \sigma(W_o \cdot [h_{t-1}, x_t] + b_o) \\ h_t &= o_t * \tanh(c_t) \end{aligned} \quad (1)$$

In LSTM, σ is the sigmoid function and \tanh is the hyperbolic tangent function; W and b represent the weight matrix and bias vector, respectively; f_t, i_t, o_t are internal gate variables of the cell. Fig. 2 gives a diagrammatic illustration of an LSTM cell. In general, the recurrent layer (or LSTM layer) is connected to non-recurrent layers such as fully connected layers so that the cell output propagates further. We denote the remaining layers with a function $\phi_2 : Y' \rightarrow Y$. Meanwhile, there can be feedforward layers connecting to the RNN layer, and we let it be another function $\phi_1 : X \rightarrow X'$. As a result, the RNN

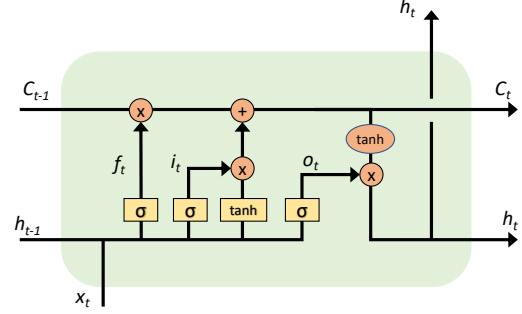


Fig. 2: LSTM Cell

model that accepts a sequence of inputs x_1, \dots, x_n can be modeled as a function φ such that

$$\varphi(x_1 \dots x_n) = \phi_2 \cdot \psi\left(\prod_{i=1}^n \phi_1(x_i)\right) \quad (2)$$

A. LSTM cell structure

The processing of a sequential input $x = \{x_t\}_{t=1}^n$ with an LSTM layer function ψ , i.e., $\psi(x)$, can be characterised by gate activations $f = \{f_t\}_{t=0}^n$, $i = \{i_t\}_{t=0}^n$, $o = \{o_t\}_{t=0}^n$, cell states $c = \{c_t\}_{t=0}^n$, and outputs $h = \{h_t\}_{t=0}^n$. We let $S = \{f, i, o, c, h\}$ be a set of structural components of LSTM, and use variable s to range over S .

B. LSTM sequential structure

Each s represents one aspect of the concrete status of an LSTM cell. To capture the interactions between multiple LSTM steps, temporal semantics are often used by human operators to understand how LSTM performs [32]. Test metrics in this paper will rely on the structural information such as *aggregate knowledge* $\xi_t^{h,+}$, $\xi_t^{h,-}$ and *remember rate* $\xi_t^{f,avg}$, as explained below, and their temporal relations.

Output h is seen as short-term memory (as opposed to c for long-term memory) of LSTM. It is often used to understand how information is updated, either positive or negative according to the value of h_t . Thus, we have

$$\xi_t^{h,+} = \sum \{h_t(i) \mid i \in \{1, \dots, |h_t|\}, h_t(i) > 0\} \quad (3)$$

$$\xi_t^{h,-} = \sum \{h_t(i) \mid i \in \{1, \dots, |h_t|\}, h_t(i) < 0\} \quad (4)$$

Intuitively, $\xi_t^{h,+}$ ($\xi_t^{h,-}$) represents the positive (negative) *aggregated* knowledge regarding short-term memory.

The forget gate f is a key factor for long memory in LSTM, as it controls whether the aggregate information can be passed on to the next (unfolded) cell or not. The portion of information passed is then measured by $\xi_t^{f,avg}$ as follows.

$$\xi_t^{f,avg} = \frac{1}{|f_t|} \sum_{i=1}^{|f_t|} f_t(i) \quad (5)$$

Example 2.1: Fig. 3 presents a set of visualisations to the temporal update of the abstracted information. In particular,

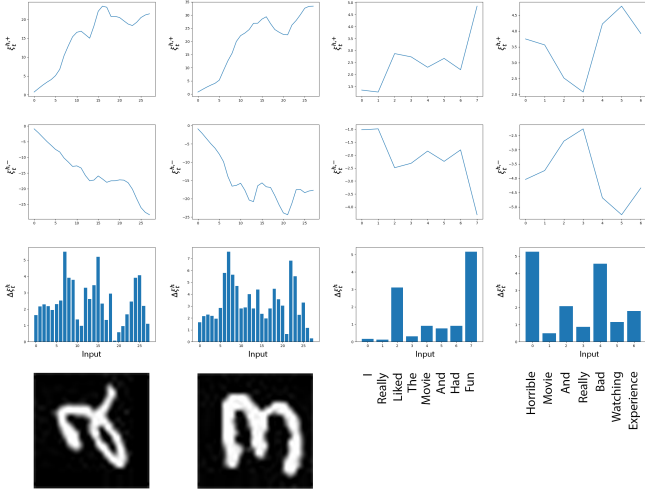


Fig. 3: Four examples to show how positive and negative elements of output vectors represent the information in MNIST and IMDB models. The x-axis includes the inputs (bottom row) and the y-axis includes $\xi_t^{h,+}$ (top row), $\xi_t^{h,-}$ (second row) and $\Delta \xi_t^h$ (third row) values. In MNIST, each column of pixels corresponds to a step in LSTM and in the IMDB model each step represents a word in the movie review.

the top row contains curves for $\xi_t^{h,+}$ and the second row contains curves for $\xi_t^{h,-}$, changed with respect to the time. The third row visualises the evolution of step-wise change information $\Delta \xi_t^h$, which will be introduced later.

Let $\mathcal{A} = \{+, -, avg\}$ be a set of symbols representing the abstraction functions as in Eq. (3-5). The above can be generalised to work with any $s \in \mathcal{S}$ and $a \in \mathcal{A}$. For $\xi_t^{s,a}$, once given a fixed input x , we may write $\xi_{t,x}^{s,a}$.

III. TEST COVERAGE METRICS FOR LSTM

In this section, we formulate a set of coverage metrics to test LSTM models. The metrics are based on not only the values of $\xi_t^{s,a}$ for $s \in \mathcal{S}$ and $a \in \mathcal{A}$ but also their step-wise and bounded-length temporal relations. Coverage metrics define test conditions that are to be validated by test cases, whose generation method will be discussed in Section IV.

a) Boundary Coverage (BC): Boundary values are of particular interest in software testing, as they often indicate extreme behaviours. We define BC to cover test conditions that hit boundary values of LSTM data flow as follows.

$$\{\xi_t^{s,a} \geq v_{max}, \xi_t^{s,a} \leq v_{min} \mid t \in \{1..n\}\}$$

where $s \in \mathcal{S}$ and $a \in \mathcal{A}$. The thresholds v_{max} and v_{min} represent its maximum and minimum values. The values can be estimated by e.g. measuring over the training dataset. For example, we can let v_{max} be the largest value in the set $\{\xi_{t,x}^{s,a} \mid t \in \{1..n\}, x \text{ is in training dataset}\}$.

Example 3.1: A test condition $\xi_t^{i,avg} > 0.9$ requires that the value $\xi_t^{i,avg}$ is greater than the designated threshold 0.9. As shown in Eq. 1, input gate i controls how much information contained in the input is received by the network. $\xi_t^{i,avg} = 0$ implies no input information is added to the long term memory

c , while $\xi_t^{i,avg} = 1$ implies all the input information is added to the long term memory c . This test condition exercises LSTM's learning ability on the input at time t .

b) Step-wise Coverage (SC): SC targets the temporal changes between connected cells. We use $\Delta \xi_t^s = |\xi_t^{s,+} - \xi_{t-1}^{s,+}| + |\xi_t^{s,-} - \xi_{t-1}^{s,-}|$ to outline the maximum change of the structural component $s \in \mathcal{S}$ at time t . For example, $\Delta \xi_t^h$ is for the change of short-term memory at time t .

Then, test conditions from SC are as follows.

$$\{\Delta \xi_t^s \geq v_{SC} \mid t \in \{1..n\}\}$$

where $s \in \mathcal{S}$. The above set defines test conditions such that an LSTM's step-wise update exceeds certain threshold v_{SC} . The threshold v_{SC} can be obtained by e.g., measuring over the training data. For example, we can let v_{SC} be the largest value in $\{\tau \cdot \Delta \xi_{t,x}^s \mid t \in \{1..n\}, x \text{ is in training dataset}\}$ for $\tau \in (0, 1]$ a pre-specified constant.

Example 3.2: Consider a sentiment analysis example in Fig. 3, where an LSTM network is trained to classify the sentiment (positive or negative) of movie reviews. After a preprocessing step, we can decide that the v_{SC} threshold in this model is 3. That is, a test condition $\Delta \xi_t^h > 3$ means that at time step t , there is a drastic change to the output h . As in Fig. 3, now let us consider two inputs "horrible movie and really bad watching experience" and "I really liked the movie and had fun". We can clearly see the difference between the SC memory values of $\Delta \xi_t^h$ at different steps, i.e., different words. It turns out that the sensitive words such as "like", "horrible", "fun" trigger greater $\Delta \xi_t^h$ values than non-sensitive words such as "movie", "really", and "had".

c) Temporal Coverage (TC): The power of LSTM comes from its ability to memorize values over arbitrary time intervals. Ideally, test metrics need to ensure that the temporal patterns of memory updates are fully exploited. This complex task is essentially a time series classification problem and is intractable. In the following, we define coverage and test conditions to exploit temporal patterns of bounded length. We remark that, unlike temporal logic for dynamic systems [12] where the temporal relation can be infinite, the temporal relations in RNNs are always finite, because the input is of finite size. Therefore, a bounded-length temporal relation does not lower the expressiveness of the test conditions.

First of all, we define a symbolic representation for any temporal curve over $\xi^{s,a} = \{\xi_t^{s,a}\}_{t=1}^n$. We start from discretising $D(\xi^{s,a})$ – the domain of $\xi^{s,a}$ – into a set Γ of sub-ranges. This discretisation can refer to the distribution of $\xi_t^{s,a}$, which can be estimated by conducting probability distribution fitting over the training dataset. Then, every time series $\{\xi_t^{s,a}\}_{t=0}^n$ can be represented as a sequence of symbols in the standard way. An example is illustrated in Fig. 4, where the continuous space of $\xi^{s,a}$ is split into three sub-ranges $\Gamma = \{a, b, c\}$.

Subsequently, we define test conditions from TC to cover a set of symbolic representations across multiple time steps $[t_1, t_2] \subseteq [1, n]$ as follows.

$$\{k_0 k_2 k_{t_2-t_1} \mid k_j \in \Gamma, j \in [0, t_2 - t_1]\} \quad (6)$$

Essentially, TC requests the testing to meet a set of temporal patterns for a specific time span $[t_1, t_2]$.

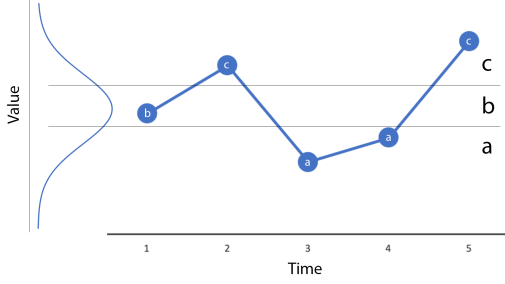


Fig. 4: Illustration of projecting a temporal curve into a sequence of symbols. In this example, a Gaussian distribution over the possible values is assumed (or estimated with the training dataset) and then the sizes of sub-regions in Γ are determined by equivalently splitting the region under curve.

Example 3.3: Fig. 3 includes two curves for each input for a certain time span. The curve in the top row is for $\xi_t^{h,+}$ and the one in the second row is for $\xi_t^{h,-}$. Combining the two curves, we can see a clear illustration on the information processing of LSTM for each input. Moreover, the time series in Fig. 4 can be symbolically represented as *bcaac* with $\Gamma = \{a, b, c\}$.

IV. COVERAGE GUIDED TEST CASE GENERATION

Coverage metrics in Section III define test conditions that may request particular patterns of long-term or short-term updates of abstracted information across multiple LSTM time steps. In this section, we present our method of generating a test suite, i.e., a set of test cases. Given an LSTM network and a specific test metric, once a test suite is generated, the **coverage rate** is the percentage of test conditions that have been satisfied. To efficiently achieve high coverage rate, we propose a coverage guided LSTM testing approach as that is outlined in Fig. 5. We remark that, although we focus on LSTM in this paper, this approach can be easily extended to work with other classes of RNNs with customized recurrent layer structure, including both the test metrics and the test case generation.

The test case generation is detailed in Algorithm 1. It starts from a corpus of seed inputs \mathcal{T}_0 . Initially, the test suite \mathcal{T} contains only inputs from \mathcal{T}_0 (Line 1). New test cases are generated by mutating seed inputs. To keep the traceability of test cases for the test oracle automation (Section IV-C), we use a mapping *dict*, which maps each test case back to its origin in the seed corpus.

The main body of Algorithm 1 is an iterative loop (Lines 5–10) that continues as long as the target coverage level has not been reached (Line 4). At each iteration, a test input x is selected from the input queue (Line 5), and it is mutated following the pre-defined mutation function m (Line 6). Newly generated test inputs are added into the input corpus \mathcal{T} (Line 7), where they are further selected and queued for the next iteration. Afterwards, a misclassification condition, as well as the oracle, are called to determine whether the generated test case represents a fault (Lines 9–10).

A. Selection policies and queuing

As shown in Fig. 5, to improve the efficiency, inputs are selected according to certain policies for the Mutator engine. Not all inputs in the corpus \mathcal{T} are equivalently important, and they are ranked once added to the input queue. When sorting queuing inputs on \mathcal{T} , TESTRNN particularly prioritizes two kinds of test inputs: those that are promising in leading to the satisfaction of un-fulfilled test conditions and those that can trigger erroneous behaviours. Adversarial examples are the most well-known erroneous behaviours in deep learning. Thanks to its modular design, new selection policies can be easily integrated into TESTRNN as plug-ins.

The design of TESTRNN also features its high parallelism. The use of dynamically allocated input queues further optimises its runtime performance.

Algorithm 1: TESTRNN Algorithm

Input:

\mathcal{N} : DNN to be tested
 \mathcal{T}_0 : a set of seed inputs
 m : a mutation function
 α_{oracle} : oracle radius

Output:

\mathcal{T} : a set of test cases
 \mathcal{T}_{adv} : a set of discovered adversarial examples

```

1  $\mathcal{T} \leftarrow \mathcal{T}_0$ 
2  $orig \leftarrow dict()$ 
3  $orig[x] \leftarrow x$  for all  $x \in \mathcal{T}_0$ 
4 while coverage rate is not satisfied do
5    $x \leftarrow$  select an element from  $\mathcal{T}$ 
6    $x' \leftarrow m(x)$ 
7    $\mathcal{T} \leftarrow \mathcal{T} \cup \{x'\}$ 
8    $orig[x'] \leftarrow orig[x]$ 
9   if  $\|orig(x) - x'\|_2 \leq \alpha_{oracle}$  and  $\mathcal{N}(x) \neq \mathcal{N}(x')$ 
10    then
11       $\mathcal{T}_{adv} \leftarrow \mathcal{T}_{adv} \cup \{x'\}$ 
11 return  $\mathcal{T}, \mathcal{T}_{adv}$ 

```

B. Mutation policies

The core of TESTRNN test case generation is its Mutator engine. Both random and RNN specific mutation policies have been implemented by the mutation function m in Algorithm 1. In the following, we discuss in details the mutation policies in TESTRNN.

a) *Random Mutation:* For problems with continuous inputs, such as MNIST handwritten image recognition, we add Gaussian noise with fixed mean and variance to the inputs and expect that the mutated inputs keep their original classifications. However, for problems with discrete inputs such as sentiment analysis on IMDB movie reviews, we define a set \mathcal{M} of mutation functions. At the beginning of a new iteration (Lines 5–10 in Algorithm 1), m is randomly instantiated by a function in \mathcal{M} . The mutation functions \mathcal{M} is problem-specific and we will provide details to those \mathcal{M} used in our experiments in Section V-A.

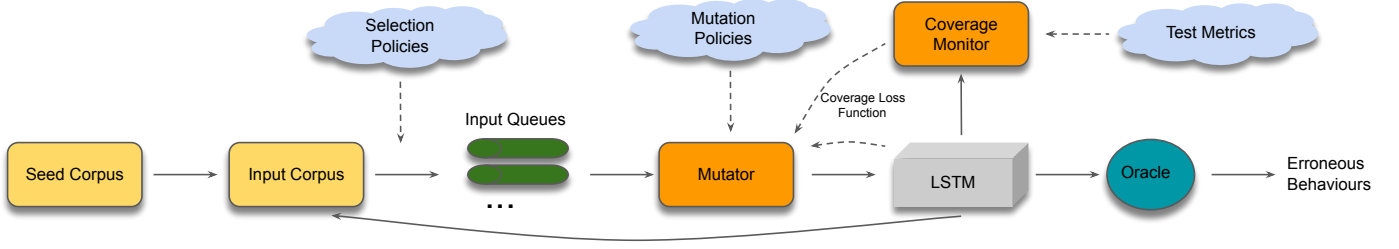


Fig. 5: TESTRNN coverage-guided RNN testing approach: Cloud shapes indicate plugged-in implementations.

b) *Targeted Mutation*: When coverage rate is difficult to improve, we may refer to a targeted mutation, which selects new test cases only when they improve over the existing test cases on some pre-defined coverage loss function. For the three classes of test conditions (BC, SC, TC) with respect to some $s \in \mathcal{S}$ and $a \in \mathcal{A}$, we define the coverage loss function as the distance to their respective targets, e.g.,

$$\begin{aligned} J_{BC}(x) &= \xi_{x,t}^{s,a} - v_{max} \\ J_{SC}(x) &= \Delta \xi_{x,t}^s - v_{SC} \\ J_{TC}(x) &= ||u_x^{[t_1, t_2]} - u_{target}||_0 \end{aligned}$$

where t, t_1, t_2 are time steps that can be inferred from the context, $u_x^{[t_1, t_2]}$ represents the symbolic representation of $\xi^{s,a}$ within time span $[t_1, t_2]$ for the input x , and u_{target} is a target symbolic representation. $||u_1 - u_2||_0$ is the Hamming distance, calculating the number of different elements between two symbolic representations u_1 and u_2 .

Intuitively, the coverage loss $J(x)$ is to estimate the distance to the satisfaction of an un-fulfilled test condition. By generating test cases with the objective of gradually minimising the loss, the targeted mutation is a greedy search algorithm.

Algorithm 2: Targeted Mutation

Input:

J : coverage loss function

n : maximum iteration number

m_{rnd} : a random mutation function

x' : a test case that is the closest to satisfy test condition

Output:

x'_{new} : a test case covering new test condition

1 $itr = 0$

2 **while** test condition has not been satisfied and $itr < n$
 do

3 $x'_{temp} \leftarrow m_{rnd}(x')$

4 **if** $J(x'_{temp})$ is closer to 0 than $J(x')$ **then**

5 $x' \leftarrow x'_{temp}$

6 $itr = itr + 1$

7 **return** x'

The targeted mutation m is shown in Algorithm 2. Candidate new test cases x'_{temp} are still generated based on random mutation (Line 3). The coverage loss function guides the generation by keeping those candidates only when they are closer to 0 than the current best x' (Lines 4-5). The procedure terminates when either the test condition is satisfied or the maximum number of iterations has reached (Line 2).

C. Test Oracle

Test oracle is usually employed to determine if a test case passes or fails. Test oracle automation is important to remove a bottleneck that inhibits greater overall test automation [5]. For our testing of LSTM networks, we employ a constraint (or more broadly, a program) to determine whether a generated test case passes the oracle or not. A test case does not pass the test oracle suggests a potential safety loophole. It is usually for the designer (or developer) of the LSTM network to determine which constraint should be taken as the oracle, since the latter relates to the correctness specification of the network under design. In this paper, as an example to exhibit our test framework, we take the currently intensively-studied adversarial example problem [46] to design our test oracle, and remark that the test oracle in general is orthogonal to the test framework we developed in this paper.

Practically, to work with adversarial examples, we define a set of norm-balls, each of which is centered around a data sample with known label. The radius α_{oracle} of norm-balls is given to intuitively mean that a human cannot differentiate between inputs within a norm ball. In this paper, we consider Euclidean distance, i.e. L^2 -norm $||\cdot||_2$. We say that a test case x' does not pass the oracle if and only if (1) x' is within the norm-ball of some known sample x , i.e., $||x - x'||_2 \leq \alpha_{oracle}$, and (2) x' has a different classification from x , i.e., $\varphi(x) \neq \varphi(x')$. Take the definition in [45], a test case does not pass the oracle is an adversarial example. Line 9 of Algorithm 1 checks whether or not a test case passes the oracle.

Given an LSTM network and a specific test metric, once a test suite is generated, the **adversary rate** is the percentage of test cases that do not pass the oracle.

V. EVALUATION

We evaluate the proposed coverage-guided LSTM testing approach with an extensive set of experiments in order to address the following six research questions.

- **RQ1**: Why do we need to design new coverage metrics for RNNs?
- **RQ2**: What is the correlation between adversarial examples and high coverage rate?
- **RQ3**: Are the proposed test metrics useful in guiding the testing approach to test a diverse set of behaviours and find erroneous behaviours?
- **RQ4**: Can the test case generation algorithm achieve high coverage for the proposed test metrics?

- **RQ5:** What is the relation between oracle radius and the adversary rate?
- **RQ6:** Are the testing results based on the proposed test metrics helpful on making LSTM interpretable?

RQ1 is to answer the motivation of the development of our coverage metrics. **RQ2**, **RQ3** and **RQ4** seek to clarify the utility of the proposed coverage-guided testing approach from several different perspectives. In particular, **RQ2** is to understand whether or not an observation made in [28], [13], i.e., a robustness evaluation based on structural test metrics may not be a good indicator of the actual robustness of CNNs, stands in the context of RNNs and our test metrics. **RQ3** and **RQ4** are to understand the effectiveness of the two components of our testing approach, i.e., test metrics and test case generation, respectively. **RQ5** examines a detailed parameter configuration, i.e., oracle radius, of the TESTRNN. A statistical method for an answer to this research question may be utilised to compare the robustness of different models. Finally, our answer to **RQ6** shows for the first time that a deep learning testing method can be utilised to achieve a better understanding of the model. This is a step towards an important missing piece of deep learning testing, i.e., how to use the testing to improve the deep learning model? We believe a good understanding is a significant step towards the improvement.

A. Experimental Setup

1) *Evaluation Model:* Our experiments are conducted on a diverse set of LSTM benchmarks, including

- MNIST handwritten digits analysis (by LSTM) [10].
- Sentiment analysis [1] to classify IMDB movie reviews.
- Lipophilicity prediction, a biological application for drug discovery. An LSTM model is trained over a Lipophilicity dataset downloaded from MoleculeNet [51]. The input is a SMILES string (Fig. 6) representing a molecular structure and the output is its prediction of Lipophilicity.
- Video recognition to classify human actions in videos. It is a large scale VGG16+LSTM network, trained over UCF101 dataset [42]. VGG16, a CNN for ImageNet, extracts features from individual frames of a video. Then, the sequence of frame features are analysed by LSTM layer for classification.

2) *Test Metrics:* We conduct experiments on several concrete test metrics, i.e., BC (for $\xi_t^{f,avg}$), SC (for $\Delta\xi_t^h$), TC+ (for $\xi_t^{h,+}$), and TC- (for $\xi_t^{h,-}$).

3) *Input Mutation:* For MNIST model, we add Gaussian noise to input image and round off the decimals around 0 and 1 to make sure the pixel value stay within the value range.

The input to IMDB model is a sequence of words, on which a random change may lead to an unrecognisable (and invalid) text paragraph. To avoid this, we take a set \mathcal{M} of mutants from the EDA toolkit [48], which was originally designed to augment the training data for improvement on text classification tasks. The benefit of this is that, we can always ensure that the mutated text paragraphs are valid. In our experiments, we consider four mutation operations, i.e., \mathcal{M} includes (1) Synonym Replacement, (2) Random Insertion, (3)

Random Swap, (4) Random Deletion. The text meanings are reserved in all mutations.

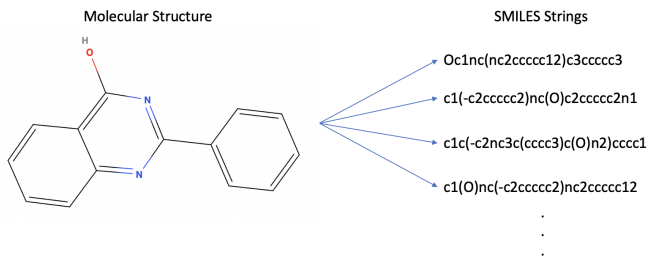


Fig. 6: The same molecular structure represented by different SMILES strings

For Lipophilicity model, we take a set \mathcal{M} of mutants which change the SMILES string without affecting the molecular structure it represents. The enumeration of possible SMILES for a molecule is implemented with the Python cheminformatics package RDkit [38]. Each input SMILES string is converted into its molfile format, based on which the atom order is changed randomly before converting back. As shown in Fig. 6, there may be several SMILES strings representing the same molecular structure. The enumerated SMILES strings will be test cases.

For UCF101 model, we add Gaussian noise to the original video frames instead of the feature input to LSTM layer. This is the large-scale model we use to evaluate our whole test framework.

4) *Oracle Setting:* Except for the experiments in Section V-D, which studies how oracle radius affects the adversarial examples, we use one fixed oracle radius for each model across all experiments. For MNIST model, we let $\alpha_{oracle} = 0.005$. For IMDB model, we let $\alpha_{oracle} = 0.05$. For Lipophilicity model, we let $\alpha_{oracle} = \infty$, suggesting that no constraint is imposed on the norm ball. Hence, the determination of adversarial example is completely based on the classification. This is because, as suggested before, the test cases are only generated from those SMILES strings with the same molecular structure. For UCF model, we let $\alpha_{oracle} = 0.1$.

All the experiments are run on a laptop with Intel(R) Xeon(R) CPU E5-2603 v4 @ 1.70 GHz and 64 GB Memory.

B. Effectiveness of Test Metrics (**RQ1**, **RQ2**, **RQ3**)

We firstly discuss the motivation of developing new test metrics for RNNs and then study the effectiveness of our test metrics from two aspects: the sensitivity of test metrics to adversarial examples, and the correlation between the metrics. This experiment considers MNIST, IMDB, and Lipophilicity models.

1) *Neuron Coverage is easy to Cover:* We consider implementing the Neuron Coverage [36], which is widely used in common DNNs, on fully connected layers of our LSTM models. In the experiments, we found that neuron coverage can be trivially achieved. For the MNIST model, on average 35 generated test cases are sufficient to cover all the test

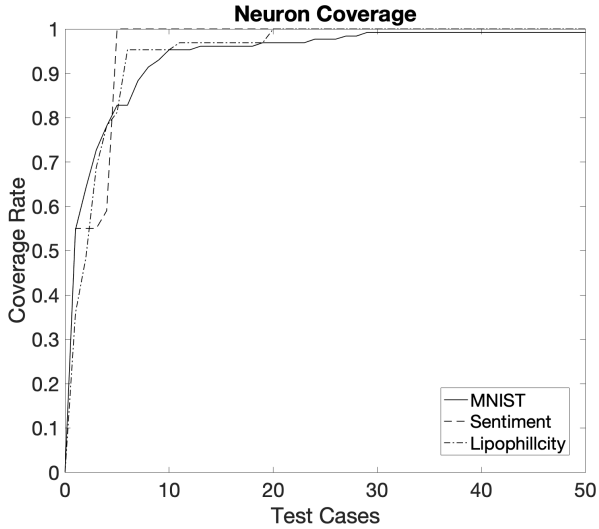


Fig. 7: The updating process of Neuron Coverage in 50 test cases.

conditions. For the IMDB model, it takes 7 test cases on average to reach 100% neuron coverage, and only 20 test cases are needed for the Lipophilicity prediction model. The detailed running results are shown in Figure 7. This shows that neuron coverage is not a suitable metric for RNNs, which also justifies the necessity of our new metrics for LSTM networks.

Answer to **RQ1**: Neuron Coverage is not suitable for robustness evaluation of LSTM models.

2) *Capturing Erroneous Behavior*: We consider the sensitivity of proposed coverage metrics to adversarial examples. We start from an *original test suite* (O) with 200 samples randomly mutated from the training dataset. Adding *adversarial examples* (A) and *normal samples* (N) to the test suite will increase the coverage rate. The adversarial examples are randomly generated from original test suite by adding Gaussian noise for misclassification, while the normal samples are also randomly mutated from original test suite but classified correctly. By considering the coverage rates on three cases: O , $O+N$, $O+A$, we can study the correlation between coverage rate and adversary rate. To make the comparison fair, we add the same amount of samples (A vs. N) to the original test suite. The experiments are repeated 5 times with different randomly-selected O . Table I shows the average results.

The best coverage rates across the three cases for each (model, metric) are presented with **bold**. We can see that, in most cases, the coverage rates for $O+A$ are higher than those for O and $O+N$. This suggests that our coverage metrics are more sensitive to adversarial inputs than normal inputs and are able to capture the erroneous behaviours of LSTM.

We remark that, since the test case generation of these RNN models are based on different random mutation strategies as described in Section IV-B, the positive correlation between high coverage rate and the adversary rate does not rely on the random mutation strategies (and therefore can be

TABLE I: coverage metrics sensitivity to adversarial examples

Test Model	No. of Test Cases	Coverage Rate			
		SC	BC	TC+	TC-
MNIST	200 (O)	0.70	0.74	0.56	0.57
	200 (O)+200 (N)	0.73	0.75	0.60	0.63
	200 (O)+200 (A)	0.79	0.87	0.61	0.64
IMDB	200 (O)	0.40	0.44	0.87	0.84
	200 (O)+200 (N)	0.46	0.51	0.90	0.87
	200 (O)+200 (A)	0.48	0.50	0.91	0.88
Lipophilicity	200 (O)	0.66	0.88	0.84	0.91
	200 (O)+200 (N)	0.71	0.88	0.88	0.91
	200 (O)+200 (A)	0.79	0.88	0.94	0.94

seen as a general conclusion).

Answer to **RQ2**: There is a strong, positive correlation between high coverage rate and the adversary rate.

Our answer to **RQ2** counters an argument made in [28], [13] for CNN testing that some simple structural metrics such as neuron coverage may not be valid indicators of robustness evaluation of CNNs. The argument was made by observing that a high coverage rate does not necessarily imply a good ability of capturing of adversarial examples, i.e., there is no strong correlation between coverage rate and adversary rate. Our experiment shows that, in the context of RNNs and our semantics-based test metrics, such a correlation can be expected. As a by-product, this conclusion suggests that our metrics can be valid estimators for RNN robustness.

3) *Complementarity of Test Metrics*: Given we have *multiple* test metrics, a natural question is whether or not these test metrics are complementary. A set of complementary test metrics (and test cases) can enhance the diversity of the testing. For the experiments, we take **minimal test suite**, in which the removal of any test case may lead to the reduction of coverage rate. The consideration of the minimality of test suite enables a fair comparison since it reduces the overlaps as much as possible. Experimental results for the three models are presented in Table II. For each model and test metric, we take a parameter, either a threshold v_{max} for BC, a threshold v_{SC} for SC, or the size $|\Gamma|$ of symbols for TC+ and TC-. In addition to the coverage rates, we also give the size of minimal test suite.

We can see from Table II that the diagonal numbers are always the greatest among those numbers on the row and the column they are in. Intuitively, if we generate a minimal test suite with a very high SC rate, the test suite does not necessarily lead to high rates of BC, TC+, or TC-. The same for BC, TC+, and TC-. This result indicates that our test metrics have few interactions in terms of test requirements. This aligns with our purpose of developing multiple test metrics for the *diversity* of testing. Actually, BC considers the values of the abstracted information, SC considers the single step change of the values, and TC considers multiple step changes of the values. They are designed to cover different aspects of the temporal semantics of RNNs.

TABLE II: Experiments for the Complementarity of Test Metrics: Comparison between Test Metrics in minimal test suite

Model	Test Metrics	Threshold or No. of Symbols	Size of Minimal Test Suite	Coverage Rate			
				SC	BC	TC+	TC-
MNIST	SC	6	21	0.821	0.464	0.219	0.312
	BC	0.85	12	0.214	0.821	0.125	0.250
	TC+	2	27	0.357	0.357	0.844	0.344
	TC-	2	27	0.250	0.429	0.219	0.844
IMDB	SC	7	263	0.908	0.768	0.875	0.812
	BC	0.73	262	0.742	0.926	0.875	0.844
	TC+	2	30	0.108	0.078	0.938	0.844
	TC-	2	30	0.108	0.078	0.844	0.938
Lipophilicity	SC	6	67	0.900	0.812	0.688	0.817
	BC	0.77	29	0.075	0.950	0.469	0.500
	TC+	2	30	0.050	0.637	0.938	0.531
	TC-	2	30	0.075	0.650	0.500	0.938

Answer to **RQ3**: The test metrics guides the testing approach in achieving the following: (a) exercise of different logics of LSTMs with a set of test metrics; (b) complementary generation of test cases between test metrics, with few redundancy.

C. Effectiveness of Test Case Generation (RQ4)

We show the effectiveness of our test case generation from the following aspects: (1) it is non-trivial to achieve high coverage rate, and (2) there is a significant percentage of adversarial examples in the generated test suite. For (1), we show that the targeted mutation (i.e., random mutation enhanced with coverage knowledge) is needed to boost the coverage rate. Three test case generation methods are considered: (SI) sampling 500 seeds input from training dataset, (RM) generating 2000 test cases from the 500 seeds by using random mutation, and (TM) generating 2000 test cases from the 500 seeds by using targeted mutation. Figure 8 demonstrates detected adversarial examples for IMDB and Lipophilicity models, and we omit other models for space limit. All experimental results are based on 5 runs with different random seeds. The results are averaged and summarised in Table III. For each test case generation method and LSTM model, we also report the number of adversarial examples in the test suite and their average L^2 -norm perturbation. The experimental settings, i.e., the threshold or number of symbols, are also given in the table. This experiment considers all four models.

We can see from Table III that, the coverage rates and the number of adversarial examples for RM are significantly higher than those of SI, that is, RM is effective in finding the adversarial examples around the original seeds. Furthermore, if we use TM, both the coverage rates and the number of adversarial examples are further increased. The above observations confirm the following two points: (1) our test metrics come with a strong bug finding ability; and (2) higher coverage rates indicate more comprehensive test. We remark that, the TC rates for UCF101 model are relatively low and harder to improve, because the mutations are made on the image frames (i.e., before CNN layers) instead of directly on the LSTM input. This shows that the adversarial examples for CNNs are

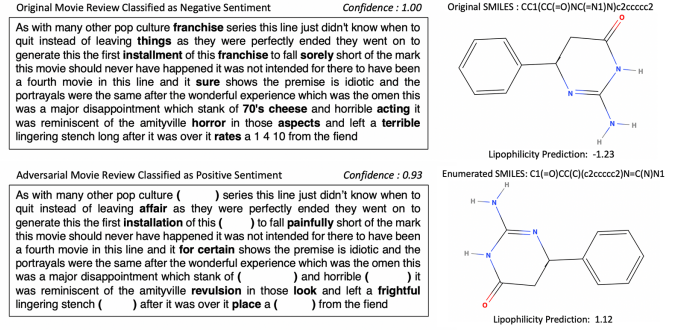


Fig. 8: Adversarial examples for IMDB (left) and Lipophilicity (right) models.

orthogonal to those of LSTMs, another evidence showing that test metrics for CNNs cannot be directly applied to RNNs.

Answer to **RQ4**: The test case generation algorithm is effective in improving both the coverage rate and the adversary rate. In particular, the targeted mutation method can be utilized to find more corner examples.

D. Impact of Oracle on Adversarial Examples (RQ5)

In the experiments so far, we adopt the default oracle radius. However, it is interesting to understand how the setting of oracle, for example the radius, may affect the quantity and quality of the adversarial examples. Here, we focus on MNSIT model to show how adversary rate and average perturbation of adversarial examples vary with different oracle radiuses. To give a clear comparison, we apply large fluctuations on input images. The hyper-parameter is set with the range of oracle radius being within $[0, 0.01]$. The experiment results are averaged over 5 different sets of seed inputs. For each set of seeds, 2,000 test cases are generated.

As shown in Fig. 9, both the quantity and the perturbation of adversarial examples increase with the oracle radius. A larger oracle radius indicates a weaker filtering ability for adversarial examples, i.e., it is easier to find adversarial examples. We can see that, adversary rate goes linearly with oracle radius, similar for the average perturbation of adversarial examples.

TABLE III: Experiments for Test Case Generation Methods

Test Model	Test Gen. Method	Test Cases	No. of Adv. Examples	Avg. Perturb. (L2 norm)	Threshold or No. of Symbols	Coverage Rate			
						SC	BC	TC+	TC-
MNIST	SI	500	0	0	$v_{sc} = 6, v_{max} = 0.85$ $ \Gamma = 2$	0.70	0.39	0.75	0.72
	RM	2000	26	1.051		0.79	0.46	0.80	0.83
	TM	2000	63	4.028		0.96	0.82	0.81	0.84
IMDB	SI	500	0	0	$v_{sc} = 7, v_{max} = 0.73$ $ \Gamma = 3$	0.68	0.71	0.48	0.50
	RM	2000	94	0.190		0.88	0.92	0.66	0.65
	TM	2000	125	0.188		0.93	0.96	0.67	0.67
Lipophilicity	SI	500	0	n/a	$v_{sc} = 6, v_{max} = 0.77$ $ \Gamma = 3$	0.24	0.82	0.58	0.54
	RM	2000	761	n/a		0.91	0.93	0.68	0.69
	TM	2000	768	n/a		0.94	0.95	0.69	0.70
UCF101	SI	20	0	0	$v_{sc} = 8, v_{max} = 0.72$ $ \Gamma = 4$	0.57	0.43	0.26	0.26
	RM	500	400	0.126		1.00	0.86	0.40	0.40
	TM	500	425	0.130		1.00	1.00	0.40	0.40

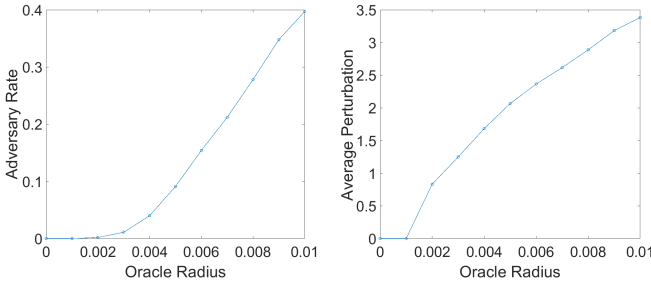


Fig. 9: The number and the average perturbations of adversarial examples against the value of oracle radius

Both curves provide an intuitive evaluation of the robustness of the model: a steeper curve, to some extent, indicates a worse robustness to the adversarial examples. Therefore, we can use these curves to compare the robustness of different LSTM models.

Answer to **RQ5**: The adversary rate increases monotonically with the oracle radius. More importantly, the curve of oracle radius vs. adversary rate, as shown in Fig. 9, can be utilised to quantify the robustness of a model and compare the robustness of two models.

E. Exhibition of Internal Working Mechanism (RQ6)

In this part, we show how to use the generated test cases from TESTRNN to understand the LSTM networks. The experiments consider visualising the learning outcome from the LSTM layer via TESTRNN results.

We define **coverage times** to denote the number of times a test condition is satisfied by running the test suite. Intuitively, coverage times represent the level of difficulty of asserting an input feature. Fig. 10 and 11 report the coverage times for each input feature. We note that, in BC and SC, each input feature x_t corresponds to a test condition on $\xi_t^{s,a}$, as in MNIST it is defined with respect to a row of pixels on the input image. More details are discussed as follows.

a) Less Active Features: Fig. 10 presents two histogram plots for SC and BC, respectively. From the SC plot (left),

we can see that the first input feature and the last few input features are not covered. This is actually expected since we split an MNIST image into rows so that each row is taken at a time step. For MNIST images, their top and bottom rows are blank, and therefore the aggregate information (and its change) is not significant enough to be over the threshold. The BC plot (right) uses a relatively large threshold 0.85. Statistically, in the first several time steps it is hard to meet this strict test condition. A reasonable explanation is that the LSTM cell in MNIST model throws away comparatively more information at the beginning. It is likely that these unnecessary information is e.g., the edges of MNIST images, as mentioned above.

For IMDB model, in Fig. 11, the plots on the bottom row show the coverage times of all 500 input features for SC and BC, respectively, while the plots on the first row show the coverage times for the last 50 input features. From the plots, we can see that no matter which coverage metric is considered, in contrast to the last 200 input features, the first 300 input features are less active and obviously “lazy” in trying to satisfy the test conditions. The reason behind this is that the inputs are padded (with trivial information as the prefix), if its size is less than 500, or truncated, if its size is larger than 500. Therefore, it is likely to see that in many test cases, the first few input features are “dead cells”.

b) Active Features: In the SC plot of Fig. 10, we can see that the test conditions for the 7th and 8th input features are easy to satisfy. This means that, for many inputs, significant changes on the output h_t are seen within this range. In other words, those input features provide significant information for the classification. In the BC plot, the long term memory c_t tends to update lazily at the end of the time series. This can be seen from the high coverage times of the value $\xi_t^{f,avg}$ over 0.85 at the last few cells.

c) Overall Analysis: If we combine SC and BC plots, the whole working process of LSTM inside the MNIST model becomes transparent. The sequential input of an image starts from the top row and finishes at the bottom row. At the beginning, the top rows of MNIST images do not contribute to the model prediction, which can be seen from the fact that they do not cause significant output changes. These less-important information is gradually thrown away from the long-term memory. When the input rows containing digits are fed

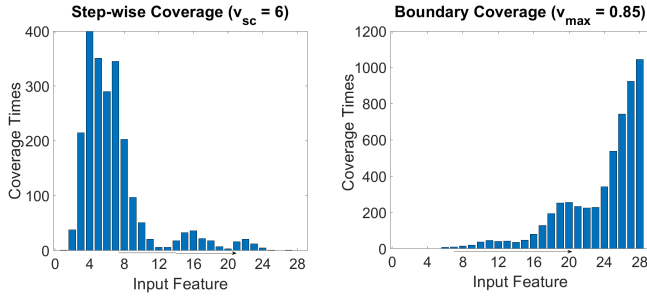


Fig. 10: 2000 test cases are used to demonstrate the coverage times of 28 features in an LSTM layer of MNIST model.

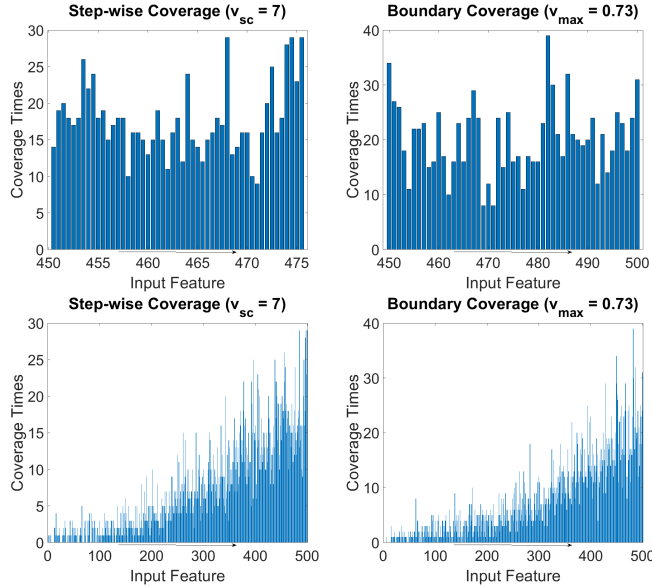


Fig. 11: 2000 test cases are used to demonstrate the coverage times of 500 input features in LSTM layer of IMDB Sentiment Analysis model. The bottom row exhibits the whole 500 input features, while the top row focuses on the last 50 input features.

to the LSTM cells, the model will start learning and the short term memory, represented by the outputs h_t , start to have strong reactions. When approaching the end of the input, which corresponds to the bottom of the digit images, LSTM has already been confident about the final classification and therefore becomes lazy to update the memory. Overall, we can see that, MNIST digits recognition is not a complicated task for the LSTM model and usually the top half of the images are sufficient for the classification.

For the IMDB model, every input feature may have an influence to the final classification. This is based on the results in Fig. 11. We take 2,000 reviews whose length are greater than 50. This is to make sure that input features between 450-500 contain real words instead of padded 0s. The plots in the top row of Fig. 11 gives the coverage times for the last 50 input features while the plots in the bottom row are for the entire 500 input features. While we can see from the bottom row that the coverage times are gradually increased, it might be because of the nature of test cases: most test cases

contain text of length much less than 500. We therefore focus on the last 50 input features, i.e., the plots in the top row. We can see that, both BC and SC test conditions in the IMDB model are randomly activated, a phenomenon that is completely different from that of MNIST results in Fig. 10. This can be explained as that the IMDB model does not have a fixed working pattern like the MNIST model. Sensitive words in a review may appear in any place of the text.

Answer to **RQ6**: The generated test suite can be utilised to understand the data processing mechanism of LSTM models. This is a step towards interpretable LSTM testing.

VI. RELATED WORK

A. Adversarial Examples for RNN

Adversarial examples have been a major safety concern for deep neural networks. The generation (or crafting) of adversarial example is an active domain. Related to this paper, we have noticed a number of works on generating adversarial examples for RNNs with respect to specific RNN tasks such as natural language processing [34], [24], [9], [54], [15], [16], [3] and automated speech recognition [18], [11], [7]. In this paper, adversarial examples are used as a proxy to evaluate the effectiveness of the proposed coverage criteria.

B. Testing feedforward neural networks

Most existing neural network testing methods focus on FNNs. In [35] the neuron coverage is proposed. Though neuron coverage is able to guide the detection of adversarial examples, it is rather easy to construct a trivial test suite to achieve very high coverage rate. Several refinements and extensions of neuron coverage are later developed in [29]. Motivated by the usage of MC/DC coverage metrics in high criticality software, in [43], a family of MC/DC variants are designed for CNNs, by taking into account the causal relation between features of different layers. Moreover, it has been shown in [43] that the criteria in [35], [29] are special cases of the MC/DC variants.

In addition to the structural coverage criteria mentioned above, metrics in [49], [4], [8] define a set of test conditions to partition the input space. Furthermore, though not being a coverage metric, the method in [26] measures the difference between training dataset and test dataset based on structural information of CNNs.

Guided by the coverage metrics, test cases can be generated by various techniques including e.g., heuristic search [53], fuzzing [33], [20], mutation [30], [47], and symbolic encoding [44], [19], etc. None of these works have considered RNNs. Please refer to [22] for a survey on techniques for the safety and trustworthiness of neural network, including formal verification [23], [25], [52], [17], [49], [40], [50], [41], [27].

C. Testing RNNs

Few works have been conducted on the development of coverage metrics for RNNs. DeepStellar [14] proposes to

abstract an RNN into a Discrete-Time Markov Chain (DTMC). The abstracted DTMC is an approximation, whose fidelity to the original RNN is unknown. Such an approximation may lead to unexpected consequences for testing, including the false positives and false negatives due to the misplacement of faulty corner cases in RNN and DTMC. Moreover, only cell states c are considered in the abstracted DTMC and the test metrics. Other essential components of RNNs, including the gates f, i, o and the output h , are not considered. As shown in our experiments, these components have their dedicated semantics and should be considered when an extensive testing is expected. They are also helpful in improving the interpretability of testing. Moreover, RNN-Test [21] considers a few test metrics to work with the structural components (output h , gate f , cell c) directly. Their test metrics can be seen as special cases of our boundary coverage. More importantly, they do not consider temporal relations, which we believe are the most essential characteristic of RNNs (as opposed to CNNs). While neither of [14], [21] release their software tools for us to compare with, we believe that the differences identified above are significant enough to make a differentiation between ours and that of [14] and that ours have included most of [21].

D. Visualisation for LSTM

For LSTMs, the processing of a sequential input $\{x_t\}_{t=1}^n$ leads to a sequence of vectors for each structural components, e.g., $\{h_t\}_{t=1}^n$ and $\{f_t\}_{t=1}^n$. These vectors are all high-dimensional, and hard to comprehend by human. To get an overview of information behind them, dimensionality reduction methods (e.g. PCA and t-SNE) have been adopted. For example, [37] employs PCA to extract the most important feature of h_t at each time step t . These methods facilitate the visualisation of RNN hidden behaviors. Our visualisation is completely different, and works by visualising the working principles of LSTM based on a set of test cases.

VII. CONCLUSIONS

In this paper, we propose a test framework for the verification and validation of recurrent neural networks. We develop a tool TESTRNN based on the test framework and validate it over a diverse set of LSTM benchmark networks. We observe that, there is a strong correlation between coverage rate and adversary rate and there is a potential of utilising test results for the interpretability of neural networks. As the future work, we are looking into the possibility of utilising the interpretations to identify the risks of the RNN models, in order to find effective means to mitigate them. Moreover, the studying of the orthogonality of adversarial perturbations between CNNs and RNNs (a phenomenon suggested in Section V-C) is also interesting: do we have a Swiss chess model [39] when connecting CNNs with RNNs?

REFERENCES

- [1] Sentiment detection with keras, word embeddings and lstm deep learning networks. <https://www.liip.ch/en/blog/sentiment-detection-with-keras-word-embeddings-and-lstm-deep-learning-networks>, 2018.
- [2] Moustafa Alzantot, Yash Sharma, Ahmed Elgohary, Bo-Jhang Ho, Mani Srivastava, and Kai-Wei Chang. Generating natural language adversarial examples. In *Proceedings of the 2018 Conference on Empirical Methods in Natural Language Processing*, pages 2890–2896, Brussels, Belgium, October–November 2018. Association for Computational Linguistics.
- [3] Moustafa Alzantot, Yash Sharma, Ahmed Elgohary, Bo-Jhang Ho, Mani B. Srivastava, and Kai-Wei Chang. Generating natural language adversarial examples. *CoRR*, abs/1804.07998, 2018.
- [4] Rob Ashmore and Matthew Hill. Boxing clever: Practical techniques for gaining insights into training data and monitoring distribution shift. In *First International Workshop on Artificial Intelligence Safety Engineering*, 2018.
- [5] E. T. Barr, M. Harman, P. McMinn, M. Shahbaz, and S. Yoo. The oracle problem in software testing: A survey. *IEEE Transactions on Software Engineering*, 41(5):507–525, May 2015.
- [6] Nicholas Carlini and David Wagner. Towards evaluating the robustness of neural networks. In *Security and Privacy (SP), IEEE Symposium on*, pages 39–57, 2017.
- [7] Nicholas Carlini and David A. Wagner. Audio adversarial examples: Targeted attacks on speech-to-text. *CoRR*, abs/1801.01944, 2018.
- [8] Chih-Hong Cheng, Georg Nührenberg, Chung-Hao Huang, and Hiro-toshi Yasuoka. Towards dependability metrics for neural networks. In *Proceedings of the 16th ACM-IEEE International Conference on Formal Methods and Models for System Design*, 2018.
- [9] Minhao Cheng, Jinfeng Yi, Huan Zhang, Pin-Yu Chen, and Cho-Jui Hsieh. Seq2sick: Evaluating the robustness of sequence-to-sequence models with adversarial examples. *CoRR*, abs/1803.01128, 2018.
- [10] François Chollet et al. Mnist hierarchical rnn. https://keras.io/examples/mnist_hierarchical_rnn/, 2015.
- [11] Moustapha Cisse, Yossi Adi, Natalia Neverova, and Joseph Keshet. Houdini: Fooling Deep Structured Prediction Models. *arXiv e-prints*, page arXiv:1707.05373, Jul 2017.
- [12] Edmund M Clarke Jr, Orna Grumberg, Daniel Kroening, Doron Peled, and Helmut Veith. *Model checking*. The MIT Press, 2018.
- [13] Yizhen Dong, Peixin Zhang, Jingyi Wang, Shuang Liu, Jun Sun, Jianye Hao, Xinyu Wang, Li Wang, Jin Song Dong, and Dai Ting. There is limited correlation between coverage and robustness for deep neural networks, 2019.
- [14] Xiaoning Du, Xiaofei Xie, Yi Li, Lei Ma, Yang Liu, and Jianjun Zhao. Deepstellar: Model-based quantitative analysis of stateful deep learning systems. In *Proceedings of the 2019 27th ACM Joint Meeting on European Software Engineering Conference and Symposium on the Foundations of Software Engineering*, pages 477–487. ACM, 2019.
- [15] Javid Ebrahimi, Daniel Lowd, and Dejing Dou. On adversarial examples for character-level neural machine translation. *CoRR*, abs/1806.09030, 2018.
- [16] Javid Ebrahimi, Anyi Rao, Daniel Lowd, and Dejing Dou. HotFlip: White-Box Adversarial Examples for Text Classification. *arXiv e-prints*, page arXiv:1712.06751, Dec 2017.
- [17] T. Gehr, M. Mirman, D. Drachler-Cohen, P. Tanskov, S. Chaudhuri, and M. Vechev. Ai2: Safety and robustness certification of neural networks with abstract interpretation. In *2018 IEEE Symposium on Security and Privacy (S&P2018)*, pages 948–963, 2018.
- [18] Yuan Gong and Christian Poellabauer. Crafting adversarial examples for speech paralinguistics applications. *CoRR*, abs/1711.03280, 2017.
- [19] Divya Gopinath, Kaiyuan Wang, Mengshi Zhang, Corina S Pasareanu, and Sarfraz Khurshid. Symbolic execution for deep neural networks. *arXiv preprint arXiv:1807.10439*, 2018.
- [20] Jianmin Guo, Yu Jiang, Yue Zhao, Quan Chen, and Jianguang Sun. DLFuzz: Differential fuzzing testing of deep learning systems. In *Proceedings of the 2018 12nd Joint Meeting on Foundations of Software Engineering, ESEC/FSE 2018*, 2018.
- [21] Jianmin Guo, Yue Zhao, Xueying Han, Yu Jiang, and Jianguang Sun. Rnn-test: Adversarial testing framework for recurrent neural network systems. *arXiv preprint arXiv:1911.06155*, 2019.
- [22] Xiaowei Huang, Daniel Kroening, Wenjie Ruan, James Sharp, Yousheng Sun, Emese Thamo, Min Wu, and Xinpeng Yi. A Survey of Safety and Trustworthiness of Deep Neural Networks. *arXiv e-prints*, page arXiv:1812.08342, Dec 2018.
- [23] Xiaowei Huang, Marta Kwiatkowska, Sen Wang, and Min Wu. Safety verification of deep neural networks. In *CAV2017*, pages 3–29, 2017.
- [24] Robin Jia and Percy Liang. Adversarial examples for evaluating reading comprehension systems. *CoRR*, abs/1707.07328, 2017.
- [25] Guy Katz, Clark Barrett, David L Dill, Kyle Julian, and Mykel J Kochenderfer. Reluplex: An efficient SMT solver for verifying deep neural networks. In *CAV2017*, pages 97–117, 2017.

- [26] Jinhan Kim, Robert Feldt, and Shin Yoo. Guiding deep learning system testing using surprise adequacy. *arXiv preprint arXiv:1808.08444*, 2018.
- [27] Jianlin Li, Jiangchao Liu, Pengfei Yang, Liqian Chen, and Xiaowei Huang. Analyzing deep neural networks with symbolic propagation: Towards higher precision and faster verification. *Submitted*, 2018.
- [28] Zenan Li, Xiaoxing Ma, Chang Xu, and Chun Cao. Structural coverage criteria for neural networks could be misleading. In *Proceedings of the 41st International Conference on Software Engineering: New Ideas and Emerging Results*, pages 89–92. IEEE Press, 2019.
- [29] Lei Ma, Felix Juefei-Xu, Jiyuan Sun, Chunyang Chen, Ting Su, Fuyuan Zhang, Minhui Xue, Bo Li, Li Li, Yang Liu, Jianjun Zhao, and Yadong Wang. DeepGauge: Comprehensive and multi-granularity testing criteria for gauging the robustness of deep learning systems. In *ASE2018*, 2018.
- [30] Lei Ma, Fuyuan Zhang, Jiyuan Sun, Minhui Xue, Bo Li, Felix Juefei-Xu, Chao Xie, Li Li, Yang Liu, Jianjun Zhao, et al. DeepMutation: Mutation testing of deep learning systems. In *Software Reliability Engineering, IEEE 29th International Symposium on*, 2018.
- [31] Dongyu Meng and Hao Chen. Magnet: a two-pronged defense against adversarial examples. In *ACM Conference on Computer and Communications Security*, 2017.
- [32] Yao Ming, Shaozu Cao, Ruixiang Zhang, Zhen Li, Yuanzhe Chen, Yangqiu Song, and Huamin Qu. Understanding hidden memories of recurrent neural networks. In *VAST2017*, pages 13–24, 2017.
- [33] Augustus Odena and Ian Goodfellow. TensorFuzz: Debugging neural networks with coverage-guided fuzzing. In *ICML2019*, 2019.
- [34] Nicolas Papernot, Patrick D. McDaniel, Ananthram Swami, and Richard E. Harang. Crafting adversarial input sequences for recurrent neural networks. *CoRR*, abs/1604.08275, 2016.
- [35] Kexin Pei, Yinzhi Cao, Junfeng Yang, and Suman Jana. DeepXplore: Automated whitebox testing of deep learning systems. In *SOSP2017*, pages 1–18. ACM, 2017.
- [36] Kexin Pei, Yinzhi Cao, Junfeng Yang, and Suman Jana. Towards practical verification of machine learning: The case of computer vision systems. *arXiv preprint arXiv:1712.01785*, 2017.
- [37] Paulo E Rauber, Samuel G Fadel, Alexandre X Falcao, and Alexandru C Telea. Visualizing the hidden activity of artificial neural networks. *IEEE transactions on visualization and computer graphics*, 23(1):101–110, 2017.
- [38] RDKit: Open-source cheminformatics. <http://www.rdkit.org>. [Online; accessed 11-April-2013].
- [39] James Reason. *Managing the Risks of Organizational Accidents*. Ashgate, 1997.
- [40] Wenjie Ruan, Xiaowei Huang, and Marta Kwiatkowska. Reachability analysis of deep neural networks with provable guarantees. In *IJCAI*, pages 2651–2659, 2018.
- [41] Wenjie Ruan, Min Wu, Youcheng Sun, Xiaowei Huang, Daniel Kroening, and Marta Kwiatkowska. Global robustness evaluation of deep neural networks with provable guarantees for L0 norm. *arXiv preprint arXiv:1804.05805*, 2018.
- [42] Khurram Soomro, Amir Roshan Zamir, and Mubarak Shah. Ucf101: A dataset of 101 human action classes from videos in the wild. *CRCV-TR-12-01*, 2012.
- [43] Youcheng Sun, Xiaowei Huang, and Daniel Kroening. Structural coverage metrics for deep neural networks. *EMSOFT2019*, 2019.
- [44] Youcheng Sun, Min Wu, Wenjie Ruan, Xiaowei Huang, Marta Kwiatkowska, and Daniel Kroening. Concolic testing for deep neural networks. In *ASE*, 2018.
- [45] Christian Szegedy, Vincent Vanhoucke, Sergey Ioffe, Jon Shlens, and Zbigniew Wojna. Rethinking the inception architecture for computer vision. In *Proceedings of the IEEE conference on computer vision and pattern recognition*, pages 2818–2826, 2016.
- [46] Christian Szegedy, Wojciech Zaremba, Ilya Sutskever, Joan Bruna, Dumitru Erhan, Ian Goodfellow, and Rob Fergus. Intriguing properties of neural networks. In *ICLR2014*, 2014.
- [47] Jingyi Wang, Jun Sun, Peixin Zhang, and Xinyu Wang. Detecting adversarial samples for deep neural networks through mutation testing. *arXiv preprint arXiv:1805.05010*, 2018.
- [48] Jason W Wei and Kai Zou. Eda: Easy data augmentation techniques for boosting performance on text classification tasks. *arXiv preprint arXiv:1901.11196*, 2019.
- [49] Matthew Wicker, Xiaowei Huang, and Marta Kwiatkowska. Feature-guided black-box safety testing of deep neural networks. In *TACAS2018*, pages 408–426. Springer, 2018.
- [50] Min Wu, Matthew Wicker, Wenjie Ruan, Xiaowei Huang, and Marta Kwiatkowska. A game-based approximate verification of deep neural networks with provable guarantees. *arXiv preprint arXiv:1807.03571*, 2018.
- [51] Zhenqin Wu, Bharath Ramsundar, Evan N. Feinberg, Joseph Gomes, Caleb Geniesse, Aneesh S. Pappu, Karl Leswing, and Vijay S. Pande. Moleculenet: A benchmark for molecular machine learning. *CoRR*, abs/1703.00564, 2017.
- [52] Weiming Xiang, Hoang-Dung Tran, and Taylor T Johnson. Output reachable set estimation and verification for multi-layer neural networks. *IEEE Transactions on Neural Networks and Learning Systems*, 29:5777–5783, 2018.
- [53] Mengshi Zhang, Yuqun Zhang, Lingming Zhang, Cong Liu, and Sarfraz Khurshid. DeepRoad: GAN-based metamorphic autonomous driving system testing. In *Automated Software Engineering (ASE), 33rd IEEE/ACM International Conference on*, 2018.
- [54] Zhengli Zhao, Dheeru Dua, and Sameer Singh. Generating natural adversarial examples. *CoRR*, abs/1710.11342, 2017.